

Examination of reference concentration under waves and currents on the inner shelf

Guan-hong Lee¹ and W. Brian Dade²

Institute of Theoretical Geophysics, Cambridge University, Cambridge, UK

Carl T. Friedrichs

Virginia Institute of Marine Science, College of William and Mary, Gloucester Point, Virginia, USA

Chris E. Vincent

School of Environmental Sciences, University of East Anglia, Norwich, UK

Received 8 November 2002; revised 31 March 2003; accepted 12 November 2003; published 24 February 2004.

[1] We examine reference concentration using three different data sets of near-bed suspended sediment concentration observed under combined waves and currents. The data include observations made at 15 and 20 m depth off Dounreay, Scotland, UK, and observations obtained at 13 m depth off Duck, North Carolina, USA. These data accommodate different dynamic conditions (from wave-dominated conditions at Dounreay to wind-driven, current-dominated conditions at Duck) and sediment properties (median size of bed sediment ranging from 120 to 350 μm). Near-bed concentration profiles to elevations of about 80 cm were obtained using acoustic backscatter sensors with 1 cm resolution. The reference concentrations (C_r) at 1 cm were then evaluated by regressing the observed suspended sediment concentrations against a Rouse-type model. Bed shear stresses associated with each estimate of C_r were estimated using the wave-current interaction model of Grant and Madsen. Existing equations for reference concentration based on shear stress alone fail to accommodate all C_r estimates from different environments. We introduce a new empirical relationship between C_r and the product of Shields and inverse Rouse numbers. These dimensionless parameters represent the ratio of bed shear stress and submerged particle weight and the ratio of shear velocity and particle settling velocity, respectively. The new formula adjusts the amount of mobile sediment at the bed (related to the Shields number) to that available for suspension at the reference height (related to the inverse Rouse number). The new formula for reference concentration accommodates observations from different environments, suggesting that it may have wide applicability on sandy inner shelves. **INDEX TERMS:** 4558 Oceanography: Physical: Sediment transport; 3022 Marine Geology and Geophysics: Marine sediments—processes and transport; 4211 Oceanography: General: Benthic boundary layers; 4219 Oceanography: General: Continental shelf processes; 4546 Oceanography: Physical: Nearshore processes; **KEYWORDS:** reference concentration, suspension, sediment, Shields parameter, Rouse number

Citation: Lee, G., W. B. Dade, C. T. Friedrichs, and C. E. Vincent (2004), Examination of reference concentration under waves and currents on the inner shelf, *J. Geophys. Res.*, 109, C02021, doi:10.1029/2002JC001707.

1. Introduction

[2] On the inner shelf, sediment resuspension and transport typically occur as the result of the combined action of waves and currents. Many models used in shelf sediment transport applications predict the time-averaged profile of sediment concentration for combined waves and currents by

solving the steady state diffusion equation [e.g., *Smith, 1977; Sleath, 1984; Glenn and Grant, 1987; Lee et al., 2002*]. In order to achieve these predictions, two components must be prescribed. One is the amount of sediment available for suspension at a specified, near-bed elevation (the reference concentration), and the other is the vertical distribution of suspended sediment. In this paper, we are concerned with reference concentration.

[3] In a seminal paper, *Smith [1977]* related the reference concentration C_r to excess shear stress S_e in the form

$$C_r = \frac{C_b \gamma_o S_e}{(1 + \gamma_o S_e)}, \quad (1)$$

¹Now at Korea Ocean Research and Development Institute, Ansan, Korea.

²Now at Department of Earth Sciences, Dartmouth College, Hanover, New Hampshire, USA.

where $S_e = (\tau_b - \tau_{cr})/\tau_{cr}$, τ_b is the bed shear stress, τ_{cr} is the critical shear stress for the bed material with characteristic grain size d_s , C_b is the relative concentration of sediment in the bed ($\cong 0.65$), and γ_o is a dimensionless resuspension coefficient. The seabed shear stress, τ_b , is related to the shear velocity $u_* = (\tau_b/\rho)^{1/2}$, where ρ is the water density.

[4] Equation (1) is based on an expression first proposed by *Yalin* [1963] and extended by *Smith* [1977] to accommodate the physical constraint that C_r can only approach (and not exceed) C_b as excess shear stress S_e becomes very large. Under typical conditions, however, $\gamma_o S_e \ll 1$, and equation (1) is approximately given by

$$C_r = C_b \gamma_o \left(\frac{u_{*sf}^2 - u_{*cr}^2}{u_{*cr}^2} \right), \quad (2)$$

where u_{*sf} and u_{*cr} are skin-friction and critical shear velocity for initiation of sediment motion, respectively. This approach has been widely used both under unidirectional flow in river and estuarine environments and under combined waves and currents in the coastal environment [*Madsen et al.*, 1993; *Webb and Vincent*, 1999; *Green et al.*, 2000; *Rose and Thorne*, 2001]. However, values of the crucial resuspension coefficient γ_o reported by various workers vary from 10^{-5} to 10^{-2} [*Drake and Cacchione*, 1989; *Hill et al.*, 1988; *Webb and Vincent*, 1999] and, under some conditions, decrease with increasing skin-friction shear velocity [*Vincent and Downing*, 1994; *Vincent and Osborne*, 1995].

[5] *Van Rijn* [1984] introduced a similar empirical expression between C_r and the excess shear stress, S_e , in the form

$$C_r = 0.015 \frac{d_s}{z_r} \frac{S_e^{1.5}}{D_*^{0.3}}, \quad (3)$$

where z_r is the height at which the reference concentration is measured and D_* is the particle parameter ($= d_s[(s-1)g/\nu^2]^{1/3}$, where g is the acceleration of gravity, ν is kinematic viscosity, and s is the density of sediment, ρ_s , relative to sea water, ρ). *Rose and Thorne* [2001] examined equation (3) using sediment concentration data collected in an estuary and reported that predictions by equation (3) were within a factor of two of the measurements.

[6] *Nielsen* [1986] introduced an alternative relationship between C_r and the dimensionless skin-friction Shields parameter, θ_{sf} , based on both field and laboratory data pertaining to relatively flat, mobile beds under waves. This relationship is given simply as

$$C_r = 0.005 \theta_{sf}^3, \quad (4)$$

where

$$\theta_{sf} = \frac{u_{*sf}^2}{(s-1)gd_s}, \quad (5)$$

in terms of the time-averaged quantity u_{*sf}^2 and the submerged grain weight $[(\rho_s - \rho)gd_s]$. *Black and Rosenberg*

[1991] and *Green and Black* [1999] found equation (4) to perform well under conditions of shoaling and broken waves over flat beds. Equation (4) was also found to perform well over rippled beds if the flow intensity appearing in the numerator of equation (5) was corrected to accommodate the effects of the ripples [*Green and Black*, 1999]. However, *Webb and Vincent* [1999] found no dependence of C_r on the Shields parameter.

[7] The approaches represented by equations (1)–(5) are based on the concept that relative fluid shear stress alone determines the amount of near-bed sediment available for suspension at a finite elevation z_r above the bed. If z_r is chosen inappropriately, however, then the dynamics governing the vertical structure of the suspended sediment must be considered [*Van Rijn*, 1984]. Even more fundamentally, we suggest that not all mobile sediment is available for suspension. In this paper, we address these issues by introducing the inverse Rouse number which represents the ratio of the skin friction velocity u_{*sf} and the characteristic settling velocity w_s of bed material.

[8] In the next section, we develop these perspectives in more detail. Three data sets of suspended sediment concentration encompassing different wave, current and grain size regimes are then introduced (section 3) and considered (sections 4 and 5) in the light of existing and new ideas about physical constraints on a reference concentration evaluated in consistent terms. In section 6, we conclude with a brief discussion and review of key findings.

2. Analysis

[9] Sediment particles of a given size begin to move when the characteristic shear velocity just exceeds the critical shear velocity for initiation of motion. The threshold condition for initiation of motion is given by the critical Shields parameter, θ_{cr} , and is empirically determined as [e.g., *Miller et al.*, 1977; *Dyer*, 1986; *Nielsen*, 1992]

$$\theta_{cr} = u_{*cr}^2 / [(s-1)gd_s]. \quad (6)$$

Mobile sediments enter into relatively continuous suspension, on the other hand, only if the shear velocity exceeds the characteristic settling velocity of the particles under consideration. Thus a suspension criterion can be expressed in terms of the Shields parameter and defined as [*Bagnold*, 1966; *Francis*, 1973]

$$\theta_s = w_s^2 / [(s-1)gd_s]. \quad (7)$$

[10] Figures 1a and 1b show the threshold conditions for incipient motion and suspension in terms of the Shields parameter, shear velocity and settling velocity [*Allen*, 1985; *Dyer*, 1986; *Nielsen*, 1992]. Two regimes of particle transport at near-critical conditions are indicated. For very fine sand (62–125 μm), values of the Shields parameter required for suspension, θ_s , are less than the values required for initiation of motion, θ_{cr} . As a result, very fine sand enters directly into continuous suspension transport upon mobilization, and equations (2)–(4) can be expected to provide a reasonable prediction of the reference concentration.

[11] In contrast, θ_s is greater than θ_{cr} for sediment with a characteristic diameter in excess of 100–200 μm , and

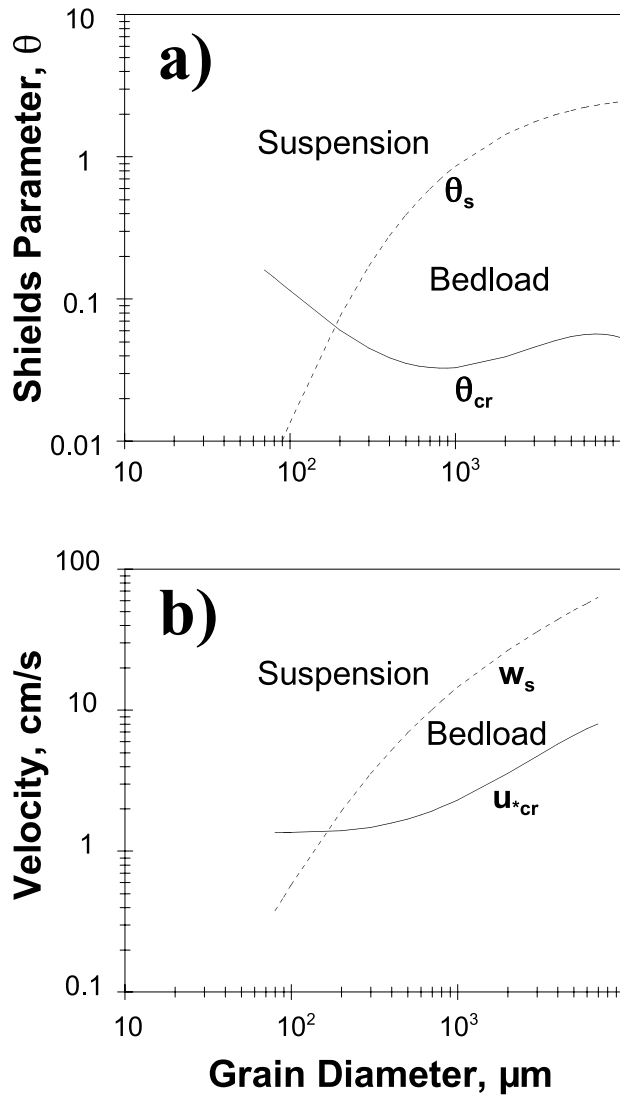


Figure 1. (a) Values of the Shields parameter required for the initiation of motion and initiation of suspension as a function of quartz grain diameter. (b) Corresponding values of critical shear velocity and settling velocity required for initiation of motion and suspension, respectively. See color version of this figure in the HTML.

thus material in this larger size range is typically transported as bed load by means of hops, rolls and saltation over the bed upon mobilization. The mobilized sediment enters into suspension only when the fluid force exceeds the settling velocity of the material. We propose that, in natural sediments comprising a range of sizes spanning $100 \mu\text{m}$, only a fraction of the total amount mobilized is actually available for suspended sediment transport and thus should be included in the reference concentration C_r .

[12] A formal statement of our ideas is as follows. The amount of sediment available for suspension depends upon the forces of fluid flow and the resistance of the particle to that flow. Previous analyses have identified a suite of key, dimensionless parameters that should be considered [Liu, 1958; Collins and Rigler, 1982]. These parameters are (1) the grain Reynolds number $Re = u_* d_s / \nu$; (2) the inverse Rouse number

$S = u_* / w_s$; and (3) the Shields parameter introduced in equation (5).

[13] Only two parameters are required when considering initiation of sediment because one is not an independent variable, but a function of other two parameters. Yalin [1963] considered the equality between the grain weight,

$$G = \alpha_f (\rho_s - \rho) g d_s^3, \quad (8a)$$

and the flow resistance, R , of a uniformly falling grain

$$R = f (w_s d_s / \nu) \rho d_s^2 w_s^2, \quad (8b)$$

where α_f is a constant. The equality gives

$$\bar{f} \left(\frac{w_s d_s}{\nu} \right) \frac{\rho w_s^2}{(\rho_s - \rho) g d_s} = 1; \quad (8c)$$

that is,

$$\bar{f} \left(Re \frac{w_s}{u_*} \right) \theta_{sf} \left(\frac{w_s}{u_*} \right)^2 = 1, \quad (8d)$$

where $\bar{f} = f / \alpha_f$. From equation (8d) it is evident that

$$u_* / w_s = \bar{f} (Re, \theta_{sf}). \quad (8e)$$

Therefore the inverse Rouse number is conventionally ignored [Liu, 1958; Yalin, 1963]. We suggest instead that in the light of the perspectives developed above, it is more sensible to neglect the grain Reynolds number but include the inverse Rouse number:

$$C_r = \varphi (u_* / w_s, \theta_{sf}). \quad (9)$$

In the following section we evaluate $\varphi (u_* / w_s, \theta_{sf})$ empirically.

3. Data and Environmental Conditions

[14] To examine appropriate reference concentrations applicable over wide-ranging dynamic conditions and sand sizes, we employed three data sets. Two data sets were collected at 15 and 20 m depth on the inner shelf off Dounreay, Scotland during 1997 and 2001, and one data set was obtained at 13 m depth during 1996 on the inner shelf off Duck, North Carolina, USA. Data acquired at 15 and 20 m depth off Dounreay are referred to as DY97 and DY01, respectively, while data obtained from Duck are referred to as DK96 hereafter. Table 1 summarizes environmental and experimental characteristics for the three experiments. The Duck site is strongly influenced by both waves and wind-driven currents, while the Dounreay site is characterized as a wave-dominated environment. The median grain size of bed sediment is $120 \mu\text{m}$ at Duck, and is 350 and $290 \mu\text{m}$ at 15 and 20 m depth at Dounreay, respectively. The Duck data are described in more detail by Lee *et al.* [2002, 2003].

[15] Figure 2 shows time series of environmental conditions for the three experiments including mean current velocity (u_c), near-bed orbital velocity (u_b), wave period

Table 1. Characteristics of the Three Data Sets

Data	DY01	DY97	DK96
Site	Dounreay, Scotland, UK	Dounreay, Scotland, UK	Duck, North Carolina, USA
Year	2001	1997	1996
Depth, m	20	15	13
Median size of bed sediment, μm	290	350	120
w_s , cm s^{-1}	3.7	4.8	1.0
u_{*cr} , cm s^{-1}	1.38	1.46	1.22
Flow sensor			
Type	Nortek Vector	EMCM	EMCM
Height, cm	30	40	98
Sample rate, Hz	5	5	1
Sample duration, min	7	9	12
Sampling interval, hours	1.5	1.5	2
ABS			
Acoustic frequency, MHz	2	2	2
Height, cm	80	82	88
Sample rate, Hz	5	2.5	5
Sample duration, min	7	4	12
Sampling interval, hours	1.5	1.5	2
Mean u_b , cm s^{-1}	16.7	18.9	19.0
Mean u_c , cm s^{-1}	9.5	9.5	14.0

(T), and shear velocities (u_{*sf} , u_{*cw} and u_{*c}). Estimation of shear velocities via the wave-current interaction model of *Grant and Madsen* [1986] follow the methods described by *Lee et al.* [2002]. The skin-friction components, u_{*sf} , is the shear velocity responsible for mobilization of sediment particles at the bed; u_{*cw} is the amplitude of shear velocity due to the combined effect of waves and currents inside the wave boundary layer, and u_{*c} is wave-averaged shear velocity just above the wave boundary layer.

[16] The environmental conditions during Dounreay 1997 and 2001 are similar in that currents were driven mainly by tides. Current speed approached 25 cm/s during spring tides, but intervals of relatively high wave energy and significant sediment transport occurred during neap tides. Thus the Dounreay site is characterized as wave dominated. In contrast, the Duck site was subject to an extratropical storm during the experiment. Mean currents were dominated by the wind-driven component, and the maximum reached up to 50 cm/s. During all three experiments considered here, the maximum near-bed wave orbital velocity exceeded 60 cm/s. The current contribution to sediment suspension was very weak at Dounreay, but played a significant role in suspending sediment during the storm event at Duck [*Lee et al.*, 2002].

4. Determination of Reference Concentration From ABS Measurements

[17] The ABSs were mounted at a nominal elevation above the bed looking downward (Table 1). Range-gating the backscattered acoustic signal allowed the sediment concentration profile to be estimated at 103, 81 and 109 range bins for DY01, DY97 and DK96, respectively, with a vertical resolution of 1 cm. The sampling rate, sample duration and sample intervals are tabulated in Table 1. A detailed description and theory of the ABS technique can be found in the work of *Thorne et al.* [1993].

[18] The ABSs were calibrated in a laboratory tank at the University of East Anglia using sand collected in a passive

sediment trap fixed to one of the legs of the deployment frames or using sand taken from the bottom by divers at the beginning of the experiment. During calibration, the backscatter signals 54 cm below the ABS transducers were inverted to obtain suspended sediment concentration. Figure 3 compares ABS measurements to suction samples collected during the laboratory calibrations.

[19] In order to determine reference concentration from observed concentration profiles, the bed level must be identified. The distance to the seabed during the field experiment rarely corresponds to the nominal seabed range chosen during the instrumentation setup because of passage of bed forms and settling of the frame during the experiment. We used the method of *Green and Black* [1999] to determine the seabed position for each burst. The burst-averaged concentration profiles usually exhibit an apparent, strong acoustic signal extending below the real bed position due to the ABS response to the very strong sound reflection at the surface of the bed. Above the strongest return there exists a break-in slope on a semilog plot of range from the ABS against concentration (Figure 4). The break-in slope

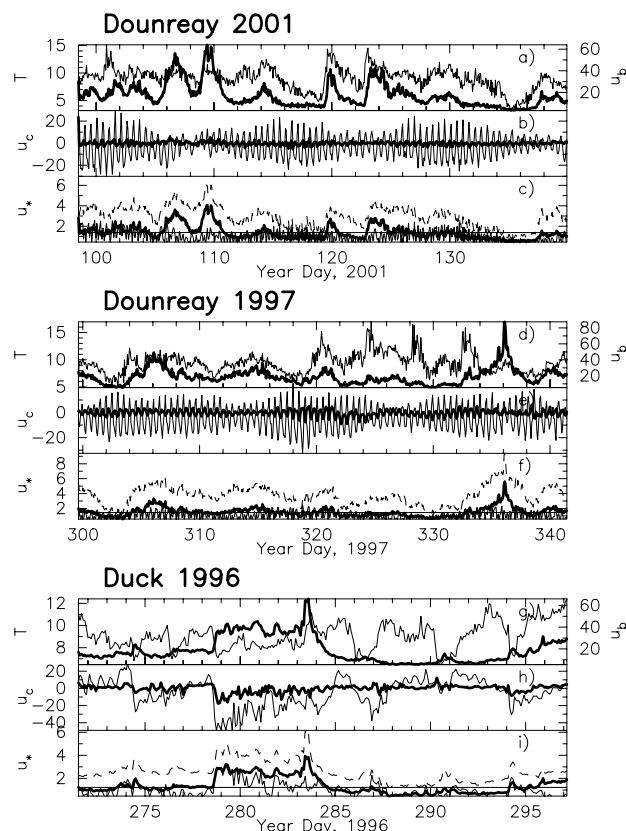


Figure 2. Time series of the environmental conditions during the three experiments considered here (Dounreay 2001, Dounreay 1997, and Duck 1996). (a, d, and g) The thick line shows near-bed wave orbital velocity, u_b ; the thin line shows wave period, T . (b, e, and h) The thick line shows the along-shore component of current velocity; the thin line shows the cross-shore component of current velocity. (c, f, and i) The thick line shows u_{*sf} ; the thin solid line shows u_{*c} ; and the thin dashed line shows u_{*cw} . See color version of this figure in the HTML.

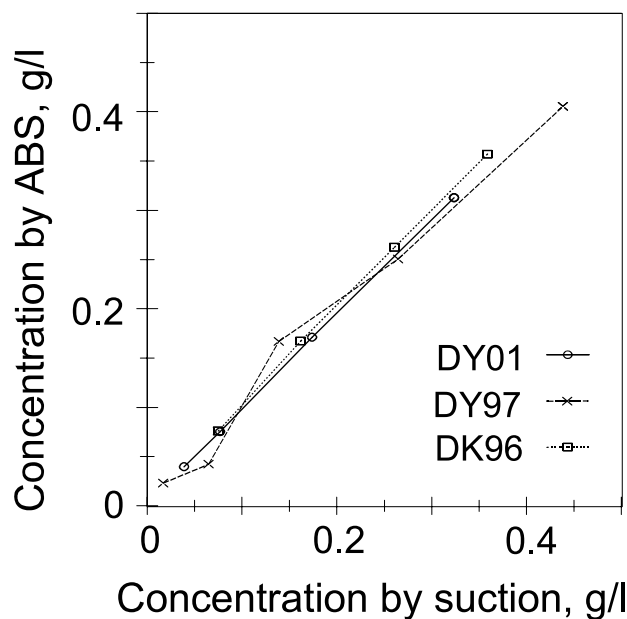


Figure 3. Comparison of concentrations measured by suction and ABS. DY01, DY97, and DK96 represent data for Dounreay 2001, Dounreay 1997, and Duck 1996, respectively. See color version of this figure in the HTML.

point is taken as the lowest echo uncontaminated by backscatter from the seabed. The vertical and horizontal arrows in Figure 4 indicate bed level and a measurement point 1 (± 0.5) cm above the bed (ab hereafter), respectively. The concentration profiles in Figure 4 are from the first burst after the initial frame deployment in each experiment.

[20] The ABS data include periods of no or little suspension. In order to ensure sufficiently strong energy conditions to suspend sediment, we screened the ABS data based on how well the suspension in the lowest 20 cm fit a one-layered Rouse-type equation. The regression model used here is expressed as

$$C = C_r(z/z_r)^{-P}, \quad (10)$$

where P is the Rouse parameter ($= w_s/\kappa u_*$) and $\kappa \equiv 0.4$ is von Karman's constant. The characteristic shear velocity, u_* , can be either u_{*c} or u_{*cw} depending on dynamical flow conditions [Lee *et al.*, 2002, 2003]. The use of a one-layered Rouse-type equation in regression analysis of near-bed ABS concentration is consistent with previous observations that has shown the inferred eddy diffusivity profile to increase linearly close to the bed [Vincent and Downing, 1994; Sheng and Hay, 1995; Vincent and Osborne, 1995; Lee *et al.*, 2002, 2003], and that separate slopes to the concentration profile associated with u_{*c} and u_{*cw} above and within the wave boundary layer cannot be resolved using ABS.

[21] In the concentration profiles it is necessary to specify a reference height at which to define the reference concentration, C_r . Because the concentration increases rapidly toward the bed, the reference height must be defined very close to the bed. If the reference height is taken at $z_r = 0$, however, the diffusion equation predicts infinite concentration. Therefore it has been commonly assumed that the

reference concentration equals the static bed concentration at a level slightly above the bed, either some small multiple of the grain size or at the height of the bed roughness length [Van Rijn, 1984; Dyer, 1986]. The reference height is set at 1 cm ab in this study for general consistency among sites. Perhaps most importantly, an approximate elevation of 1 cm simply represents the lowermost extent of direct observations. Additional analyses using reference concentrations evaluated by the regression model (10) at different reference heights indicate that the precise value chosen for z_r does not affect the overall substance of our results in the following sections (see section 6).

[22] Figure 5 shows the fraction of variance (R^2) accounted for by regression of a one-layered Rouse equation to backscatter between 1 and 20 cm ab as a function of the relative intensity of the sediment-transporting flow for each of the 1643 profiles. In Figure 5, as in Figures 6–10, the circles, crosses and squares represent values pertaining to Dounreay 2001 (DY01), Dounreay 1997 (DY97) and Duck 1996 (DK96), respectively. Figure 5 reveals that, in general, vertical profiles of suspended sediment are well described by equation (10) with relative performance increasing with the overall intensity of a flow. In the following analysis we consider the 706 cases for which $R^2 \geq 0.95$. A representative subsample of reference concentration is tabulated in Table 2 along with wave orbital velocity, wave period, current velocity, u_{*sf} , u_{*c} and u_{*cw} .

5. Examination of Existing and New Approach for Reference Concentration

[23] In this section we examine the existing formulae for reference concentration using the inferred reference con-

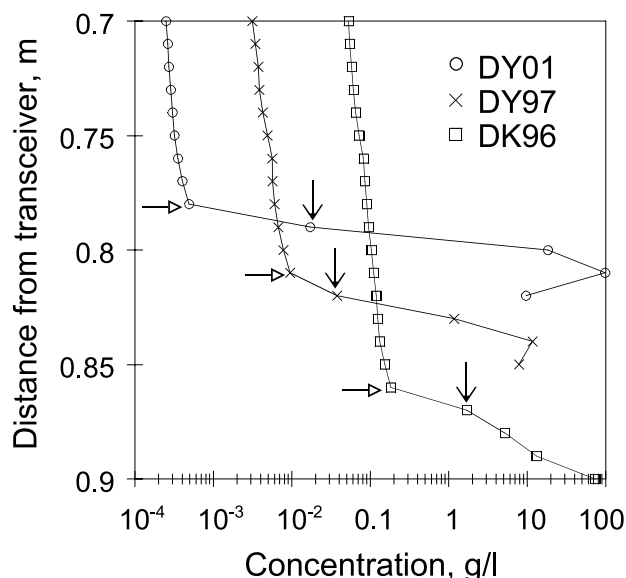


Figure 4. Representative burst-averaged ABS profiles of suspended sediment from each of the DY01, DY97, and DK96 deployments, demonstrating the criterion for determining bed level. Vertical and horizontal arrows indicate bed level and 1 cm ab, respectively. DY01, Dounreay 2001; DY97, Dounreay 1997; DK96, Duck 1996. See color version of this figure in the HTML.

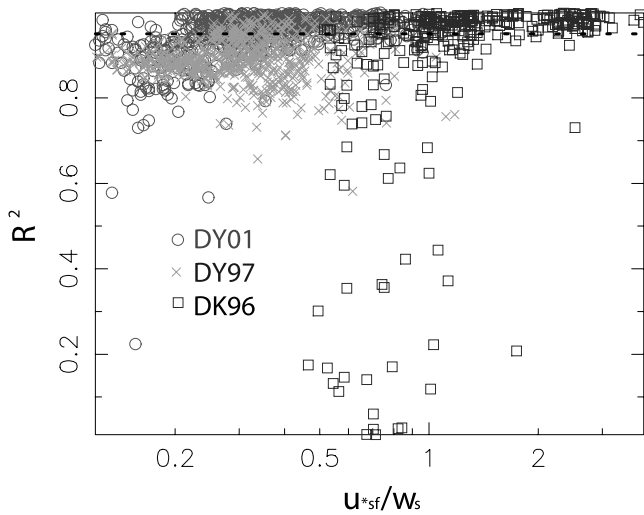


Figure 5. Fraction of variance (R^2) explained by a regression model of burst-averaged sediment concentration in g/L as a function of u_{*sf}/w_s . The dotted line indicates the criteria for data inclusion ($R^2 > 0.95$). DY01, Dounreay 2001; DY97, Dounreay 1997; DK96, Duck 1996. See color version of this figure in the HTML.

centrations in the previous section. Figure 6 shows inferred values of the reference concentration C_r at $z_r = 1$ cm ab as a function of excess shear stress. In general, equation (2) captures a proportional relationship between C_r and excess shear stress, but fails to accommodate observations from different environments satisfactorily. The empirical formulae (3) introduced by *Van Rijn* [1984] results in a pattern similar to Figure 6. The discrepancy among different data sets is concealed in the resuspension coefficient. Indeed, as shown in Figure 7, inferred values of the resuspension coefficient γ_0 (determined by forcing a best-fit to equation (2)) span the

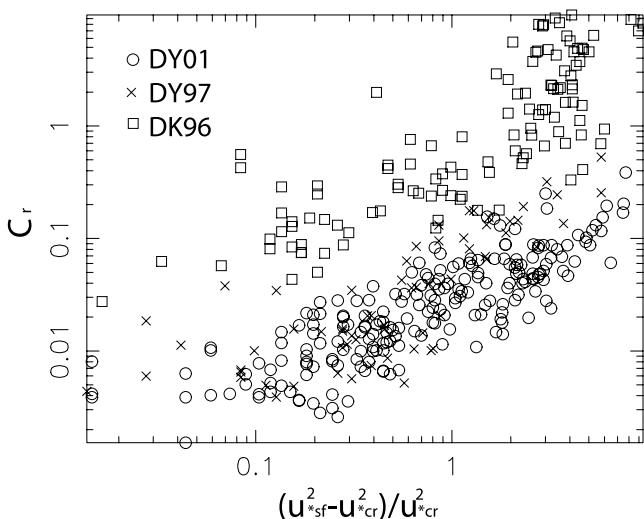


Figure 6. Reference concentration in g/L as a function of excess shear stress. DY01, Dounreay 2001; DY97, Dounreay 1997; DK96, Duck 1996. See color version of this figure in the HTML.

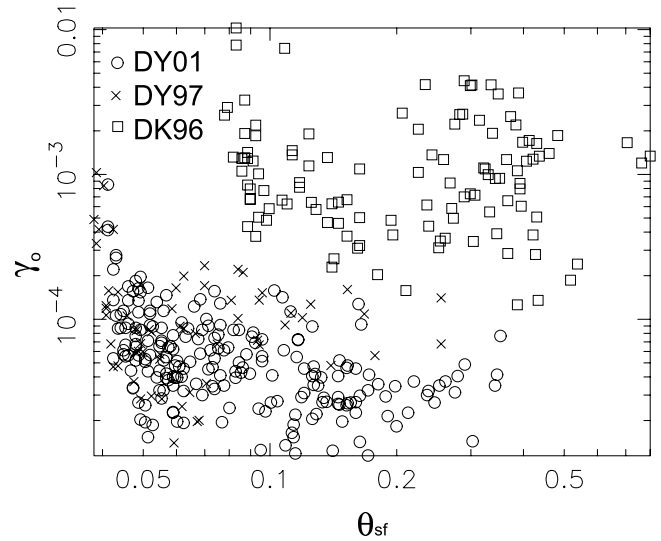


Figure 7. Resuspension coefficient as a function of the skin-friction Shields parameter. DY01, Dounreay 2001; DY97, Dounreay 1997; DK96, Duck 1996. See color version of this figure in the HTML.

range 10^{-5} to 10^{-2} and, at Dounreay at least, appear to decrease with increasing flow intensity. In order to examine the sensitivity of these results to the chosen reference height, C_r was also estimated by extrapolating observed concentration to $z_r = 2.5d_s$. As shown in Figure 8, defining $z_r = 2.5d_s$ causes the scatter associated with a plot of C_r versus excess shear stress to increase, especially for DK96. Since the discrepancy among different data sets is even worse with data estimated at $2.5d_s$, the selection of a fixed elevation above the bed is probably not responsible for the discrepancy among data sets obtained from different environments.

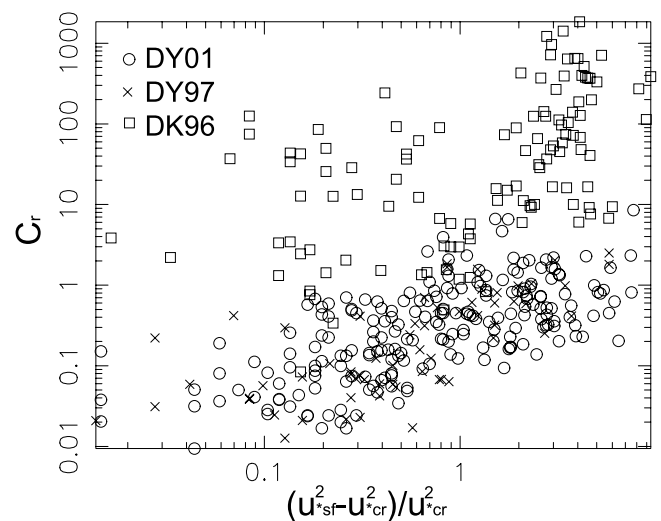


Figure 8. Reference concentration in g/L estimated at $2.5d_s$, by the regression model of equation (10) as a function of excess shear stress. DY01, Dounreay 2001; DY97, Dounreay 1997; DK96, Duck 1996. See color version of this figure in the HTML.

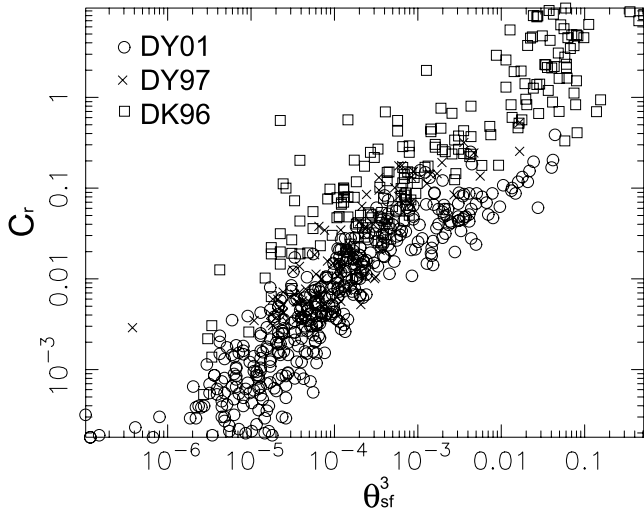


Figure 9. Reference concentration in g/L as a function of the Shields parameter raised to the power of 3. DY01, Dounreay 2001; DY97, Dounreay 1997; DK96, Duck 1996. See color version of this figure in the HTML.

[24] Figure 9 shows inferred values of the reference concentration as a function of the skin-friction Shields parameter raised to the power of 3. Nielsen's model also captures a proportional relationship between C_r and flow intensity, but fails to capture the differences among data sets to a satisfactory degree.

[25] Figure 10 displays the reference concentration in g/L as a function of the product of the Shields parameter and the inverse Rouse number. Unlike Figures 6 and 9, the dimensionless parameter accommodates all observations from different environments. The empirical relationship for the reference concentration, indicated by the solid line in Figure 10, was found by fitting

$$C_r = A \left[\theta_{sf} \frac{u_{*sf}}{w_s} \right]^B, \quad (11a)$$

where C_r in g/L is evaluated at 1 cm ab and, from regression analysis,

$$A = 2.58 \pm 1.17 \quad (11b)$$

and

$$B = 1.45 \pm 0.04, \quad (11c)$$

where the \pm values indicate the 95% confidence interval of the estimate. The regression model of equation (11) accounts for 87% of the observed variability in C_r . The success of equation (11) in accommodating a wide range of dynamic conditions and sediment properties is consistent with our initial proposal that C_r under combined waves and currents is related to relative bed shear stress (represented by θ_{sf}) adjusted for the relative intensity of sediment suspension (represented by u_{*sf}/w_s).

[26] For comparison, various combinations of three parameters considered in this study were subjected to

regression analysis. Table 3 tabulates best-fit coefficients, 95% confidence intervals, and the fraction of variance (R^2) accounted for by each regression. The case with the highest R^2 value is model V ($R^2 = 0.89$), simply because it has the largest number of best-fit parameters. Since model V is physically unrealistic and also the most complex, we reject this model. Four models have same R^2 value of 0.87, which include models II, VI, VII, and VIII. Because the relative performance of these models cannot be distinguished statistically, we chose model II, which is the simplest and is consistent with the physical reasoning behind equation (11).

6. Discussion and Conclusions

[27] The important result of this study is the introduction of a more universal, empirical equation for reference concentration for wide-ranging hydrodynamic and sedimentary environments. Although the existing formulae for reference concentration exhibited a proportional relationship (Figures 6 and 9) between shear stress and C_r , these formulae could not reconcile the observations obtained from different environments. The primary reason these existing formulae fail to accommodate all the observations is their sole dependence on threshold stress for initiation of motion of particles when a threshold condition for suspension is also required. Theoretical arguments suggest that the reference concentration is dependent on the inverse Rouse number and the grain Reynolds number, as well as the threshold stress. However, these three parameters are dependent each other and only two parameters are required when considering initiation of sediment motion and suspension. In fact, the relative performance of regression models using these parameters was statistically indistinguishable (Table 3). We recommend using the reference concentration that is a function of the product of the Shields parameter and inverse

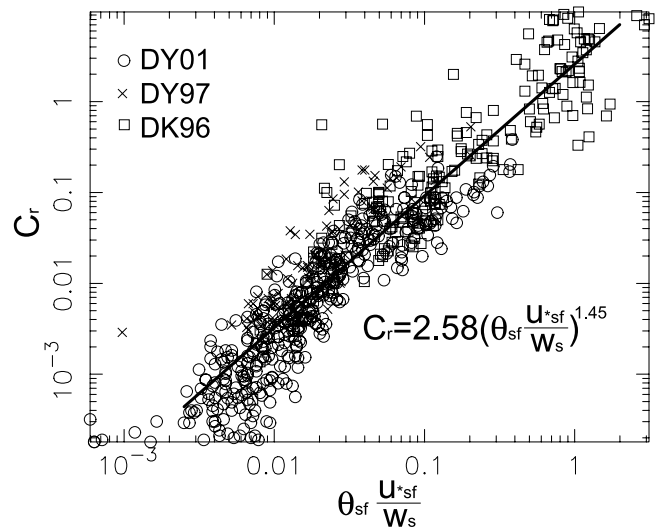


Figure 10. Reference concentration in g/L as a function of the product of the skin-friction Shields parameter and inverse Rouse number (u_{*sf}/w_s). The solid line indicates the regression of the form given by equation (11) and specified in the figure. DY01, Dounreay 2001; DY97, Dounreay 1997; DK96, Duck 1996. See color version of this figure in the HTML.

Table 2. Representative Samples of the Observed Reference Concentration

u_c	u_b	T	u_{*sf}	u_{*cw}	u_{*c}	C_r at 1 cm ab	C_r at $2.5d_s$
DY01							
20.34	10.86	9.79	1.54	3.66	1.34	0.008	0.133
18.94	23.11	9.85	1.68	3.85	2.29	0.006	0.034
22.91	8.65	9.91	1.67	3.77	1.15	0.014	0.265
22.48	9.51	9.99	1.66	3.75	1.22	0.018	0.403
14.23	28.01	8.46	1.48	3.51	2.50	0.004	0.043
18.05	28.18	10.87	1.60	3.57	2.53	0.007	0.051
29.19	5.15	9.29	2.12	4.19	0.86	0.046	1.309
24.93	16.97	10.14	1.94	3.96	1.83	0.016	0.123
22.85	11.50	8.64	1.72	4.13	1.44	0.027	0.802
17.73	8.60	7.86	1.46	3.77	1.14	0.004	0.039
24.07	11.34	10.85	1.78	3.60	1.34	0.032	0.406
25.04	12.95	9.83	1.86	3.94	1.52	0.018	0.213
20.95	12.02	9.17	1.70	3.99	1.50	0.014	0.117
30.84	21.34	10.54	2.43	4.02	2.05	0.122	1.879
19.73	11.63	9.38	1.60	3.82	1.44	0.015	0.135
23.75	14.45	10.15	1.89	3.96	1.67	0.023	0.199
16.88	19.27	9.67	1.45	3.51	1.96	0.004	0.028
40.62	1.95	11.08	2.70	4.18	0.49	0.049	0.322
40.73	14.37	9.43	2.83	4.62	1.65	0.024	0.202
52.35	6.17	9.97	3.40	5.21	1.03	0.088	0.819
39.38	9.71	9.10	2.74	4.58	1.28	0.043	0.514
41.50	8.61	10.48	2.83	4.43	1.19	0.067	1.372
29.70	6.48	10.06	2.14	3.85	0.95	0.021	0.351
27.11	2.26	9.75	1.93	3.93	0.49	0.040	0.450
20.47	7.70	8.41	1.63	4.04	1.11	0.038	0.519
31.10	9.96	8.28	2.24	4.66	1.34	0.150	4.657
52.46	6.15	10.79	3.44	5.14	1.09	0.119	0.794
64.03	13.09	11.52	4.07	5.92	1.80	0.386	8.491
57.41	6.82	9.80	3.77	5.77	1.22	0.060	0.203
31.39	8.38	9.41	2.25	4.11	1.13	0.066	1.158
35.10	13.71	9.46	2.49	4.22	1.54	0.058	2.046
22.35	5.41	9.29	1.68	3.94	0.86	0.012	0.132
20.24	7.54	12.05	1.47	3.15	0.98	0.015	0.257
20.42	14.28	10.92	1.55	3.46	1.57	0.012	0.133
22.65	17.16	11.36	1.69	3.43	1.74	0.015	0.145
35.55	10.63	13.36	2.38	3.54	1.22	0.040	1.423
35.92	9.76	12.22	2.43	3.72	1.18	0.055	0.828
34.04	7.60	13.20	2.29	3.46	0.98	0.130	6.570
21.67	11.06	12.15	1.56	3.15	1.25	0.016	0.154
37.16	8.95	12.96	2.47	3.67	1.11	0.050	0.672
36.54	7.38	12.08	2.43	3.73	0.99	0.028	0.185
40.24	11.28	11.49	2.68	4.09	1.34	0.086	0.428
29.22	10.60	10.91	2.05	3.48	1.21	0.033	0.381
31.69	10.99	11.19	2.17	3.58	1.25	0.026	0.205
27.02	16.03	10.53	1.97	3.70	1.67	0.030	0.247
21.94	3.46	10.11	1.61	3.68	0.63	0.020	0.362
28.15	11.36	9.63	2.06	4.07	1.39	0.060	1.087
20.39	2.22	10.27	1.52	3.56	0.48	0.021	0.412
17.59	12.72	9.77	1.41	3.46	1.47	0.006	0.051
16.50	20.80	9.12	1.55	3.70	2.11	0.007	0.064
18.23	20.90	10.84	1.59	3.58	2.08	0.008	0.073
16.42	12.53	9.11	1.39	3.47	1.45	0.004	0.038
DY97							
22.46	16.49	9.88	1.88	4.72	1.95	0.037	0.314
22.08	8.70	8.41	1.77	4.74	1.21	0.009	0.055
42.21	12.90	10.56	2.94	5.31	1.63	0.319	2.031
29.47	3.90	9.84	2.18	5.25	0.77	0.081	0.420
18.04	10.12	8.49	1.52	4.07	1.26	0.007	0.039
18.93	15.02	8.94	1.67	4.31	1.73	0.035	0.413
23.92	8.02	8.72	1.86	4.93	1.17	0.036	0.158
22.29	1.93	12.77	1.65	4.00	0.45	0.016	0.084
19.60	11.96	11.65	1.57	3.98	1.47	0.016	0.073
26.99	5.47	8.47	2.06	5.37	0.94	0.043	0.470
30.83	1.41	7.92	2.33	5.99	0.44	0.154	0.808
56.17	7.15	9.42	3.80	6.70	1.24	0.254	1.810
27.06	11.59	7.60	2.14	5.65	1.59	0.101	0.612
23.56	16.76	7.20	1.99	5.26	1.97	0.131	1.667
20.92	3.24	8.02	1.68	4.57	0.60	0.013	0.067

Table 2. (continued)

u_c	u_b	T	u_{*sf}	u_{*cw}	u_{*c}	C_r at 1 cm ab	C_r at $2.5d_s$
DK96							
15.19	23.11	8.07	1.35	2.90	1.64	0.148	12.678
20.13	9.20	7.45	1.48	3.18	0.84	0.448	92.404
18.26	4.96	8.11	1.32	2.88	0.52	0.075	0.761
18.79	1.06	8.17	1.30	2.84	0.16	0.169	33.911
19.14	5.03	9.40	1.31	2.55	0.50	0.084	2.440
18.84	5.45	9.23	1.30	2.59	0.53	0.115	3.442
25.47	36.35	8.15	2.02	3.30	2.18	0.179	15.064
36.89	49.01	7.42	2.86	4.51	2.96	1.119	16.569
43.19	41.70	7.64	3.17	4.94	2.79	0.697	6.745
40.31	44.36	8.46	2.74	4.14	2.68	2.788	187.536
37.89	43.83	8.67	2.61	3.94	2.61	2.191	103.738
38.50	15.75	7.96	2.53	3.96	1.30	2.140	97.112
44.24	31.67	8.47	2.83	4.29	2.17	4.889	378.422
41.39	40.44	7.81	2.77	4.28	2.56	1.629	48.148
32.28	7.07	8.09	2.14	3.43	0.70	0.832	5.986
41.38	34.75	8.23	2.73	4.17	2.28	5.718	647.650
35.14	23.14	8.78	2.43	3.71	1.68	0.665	16.627
33.16	13.08	8.85	2.13	3.30	1.06	5.561	428.270
35.62	13.92	7.76	2.37	3.77	1.17	7.997	1217.576
32.38	16.39	8.02	2.15	3.45	1.26	0.601	11.160
63.36	10.05	10.05	3.70	5.69	1.14	8.827	272.798
35.41	16.56	10.38	2.29	3.32	1.27	0.954	31.182
27.52	26.10	9.40	1.95	3.03	1.68	0.387	11.226
16.34	23.45	7.64	1.35	2.98	1.66	0.074	0.338
19.33	17.60	11.08	1.37	2.22	1.16	0.131	2.046
31.50	6.03	10.94	2.00	2.91	0.60	2.910	73.429
25.48	5.31	10.86	1.66	2.54	0.51	0.145	1.559
28.08	3.28	11.49	1.78	2.62	0.37	0.370	3.752
27.35	7.01	12.10	1.77	2.55	0.64	0.223	4.332

Rouse number because it is the simplest and consistent with our physical reasoning. In this respect, the inverse Rouse number modifies the total amount of mobile sediment (related to the Shields parameter) to account for that fraction available for suspension. As a result, the new formula accommodates all the observations from the different environments.

[28] It is important to emphasize that equation (11) pertains to a reference height of $z_r = 1$ cm. Since there is no general consensus on the most appropriate reference height, we set the reference height at the lowest level to which suspended sediment concentration could be estimated with confidence through direct observation. Other elevations could be chosen with theoretical justification. To examine the general consistency of the approach developed here, we considered different reference heights in a broader analysis. For example, concentrations at $2.5d_s$ were estimated by the regression model of equation (10) and were plotted as a function of the product of Shields parameter and inverse Rouse number (Figure 11). In contrast with the

Table 3. Best-Fit Coefficients, Confidence Interval, and Fraction of Variance (R^2) Accounted for by Each Regression

Model	Coefficient	95% Confidence Interval				R^2
		A	B	C	D	
I	$A(\theta_{sf} S Re)^B$	0.39	1.22	1.18	0.05	0.74
II	$A(\theta_{sf} S)^B$	2.58	1.45	1.17	0.04	0.87
III	$A(\theta_{sf} Re)^B$	0.21	1.34	1.28	0.11	0.45
IV	$A(S Re)^B$	0.009	2.37	1.12	0.12	0.65
V	$A\theta_{sf}^B S^C Re^D$	10^{-37}	-29	39	24×10^5	4.86 5.89 3.81 0.89
VI	$A\theta_{sf}^B S^C$	1.51	1.19	1.77	1.39	0.14 0.18 0.87
VII	$A\theta_{sf}^B Re^C$	91	2.65	-1.12	1.32	0.08 0.12 0.87
VIII	$AS^B Re^C$	0.05	3.22	0.95	1.13	0.09 0.11 0.87

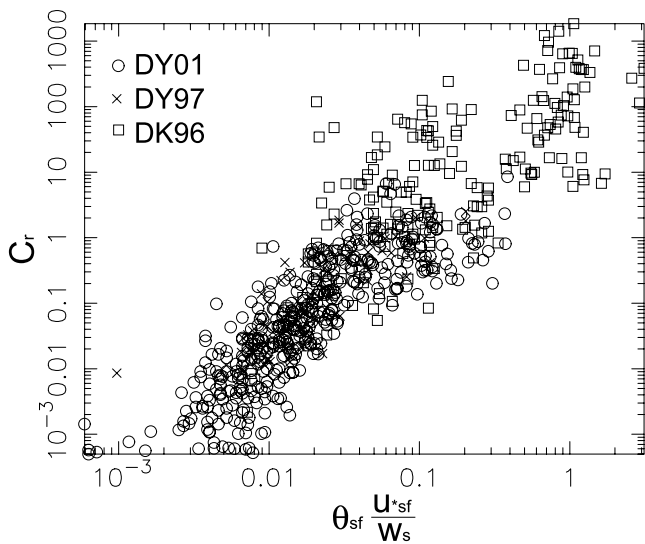


Figure 11. Reference concentration in g/L estimated at $2.5d_s$ by the regression model of equation (10) as a function of the product of the skin-friction Shields parameter and inverse Rouse number. DY01, Dounreay 2001; DY97, Dounreay 1997; DK96, Duck 1996. See color version of this figure in the HTML.

relationship shown in Figure 10, the scatter of concentration data, especially for DK96, increased ($R^2 = 0.78$). Nonetheless, the scaling parameter proposed here accommodates all estimates from wide-ranging environments. Thus the essential outcome of our analysis is robust, and independent of the exact reference height chosen. We acknowledge, of course, that improved expressions similar to equation (11) are likely to come with improved theoretical constraints on the appropriate reference height and technical ability to measure sediment concentration at that height.

[29] Recent studies suggested that the influence of bed forms must be taken into account in order to improve the model prediction on reference concentration [Webb and Vincent, 1999]. The significance of bed form influence on estimates of reference concentration was clearly demonstrated by Green and Black [1999]. In that study, they observed two groups of reference concentration that were separated by bed form types. The two bed types included large hummocks formed during energetic wave conditions and rippled bed formed during less energetic conditions. They applied a correction for flow contractions over ripples by multiplying the Shields parameter by $(1 - \pi\eta/\lambda)^2$, where η and λ are observed ripple height and ripple length. This enabled the model based on the skin-friction Shields parameter to adequately predict the reference concentration over a range of bed forms. In this study, we neglected the effect of bed forms on the magnitude of reference concentration because our data could not adequately quantify bed form variability. First, we did not observe distinct groups of reference concentration (compare Figures 6, 9, and 10) that suggested the influence of bed forms as clearly as concentration data shown by Green and Black [1999, Figure 5]. Second, there were no direct observations of bed forms collected during our experiments. Nonetheless, the potential

influence of bed forms on the magnitude of reference concentration is clear [Green and Black, 1999; Webb and Vincent, 1999]. Therefore we acknowledge that accommodation of bed form geometry will contribute to the improved performance of predictive expressions of the form given by equation (11). Such improvements are a focus of ongoing study.

[30] **Acknowledgments.** G.L. and Dounreay deployments were supported by the (UK) Atomic Energy Authority. W.B.D. was supported by the (UK) Natural Environmental Research Council. Participation by C.T.F. and field studies at Duck, NC, were supported by the (US) National Science Foundation.

References

- Allen, J. R. L. (1985), *Principles of Physical Sedimentology*, 272 pp., Allen and Unwin, Concord, Mass.
- Bagnold, R. A. (1966), An approach to the sediment transport problem from general physics, *U. S. Geol. Surv. Prof. Pap.*, 422-I, 1–37.
- Black, K. P., and M. A. Rosenberg (1991), Suspended sediment load at three time scales, in *Coastal Sediments '91, Proceedings*, pp. 313–327, Am. Soc. of Civil Eng., Seattle, Wash.
- Collins, M. B., and J. K. Rigler (1982), The use of settling velocity in defining the initiation of motion of heavy mineral grains, under unidirectional flow, *Sedimentology*, 29, 419–426.
- Drake, D. E., and D. A. Cacchione (1989), Estimates of suspended sediment reference concentration and resuspension coefficient from near-bottom observations on the California shelf, *Cont. Shelf Res.*, 9, 51–64.
- Dyer, K. R. (1986), *Coastal and Estuarine Sediment Dynamics*, 342 pp., John Wiley, Hoboken, N. J.
- Francis, J. R. D. (1973), Experiments on the motion of solitary grains along the bed of a water-stream, *Proc. R. Soc. London, Ser. A*, 332, 443–471.
- Glenn, S. M., and W. D. Grant (1987), A suspended sediment stratification correction for combined wave and current flows, *J. Geophys. Res.*, 92, 8244–8264.
- Grant, W. D., and O. S. Madsen (1986), The continental shelf bottom boundary layer, *Ann. Rev. Fluid Mech.*, 18, 265–305.
- Green, M. O., and K. P. Black (1999), Suspended-sediment reference concentration under waves: Field observations and critical analysis of two predictive models, *Coastal Eng.*, 38, 115–141.
- Green, M. O., R. G. Bell, T. J. Dolphin, and A. Swales (2000), Silt and sand transport in a deep tidal channel of a large estuary (Manukau Harbour New Zealand), *Mar. Geol.*, 163, 217–240.
- Hill, P. S., A. R. M. Nowell, and P. A. Jumars (1988), Flume evaluation of the relationship between suspended sediment concentration and excess boundary shear stress, *J. Geophys. Res.*, 93, 12,499–12,509.
- Lee, G., C. T. Friedrichs, and C. E. Vincent (2002), Examination of diffusion versus advection dominated sediment suspension on the inner shelf under storm and swell conditions, Duck, North Carolina, *J. Geophys. Res.*, 107(C7), 3084, doi:10.1029/2001JC00918.
- Lee, G., W. B. Dade, C. T. Friedrichs, and C. E. Vincent (2003), Spectral estimates of bed shear stress using suspended-sediment concentrations in a wave-current boundary layer, *J. Geophys. Res.*, 108(C7), 3208, doi:10.1029/2001JC001279.
- Liu, H. K. (1958), Closure: Mechanics of sediment ripple formation, *J. Hydrol. Div.*, 84, 5–31.
- Madsen, O. S., L. D. Wright, J. D. Boon, and T. A. Chisholm (1993), Wind stress, bed roughness and sediment suspension on the inner shelf during an extreme storm event, *Cont. Shelf Res.*, 13, 1303–1324.
- Miller, M. C., I. N. McCave, and P. D. Komar (1977), Threshold of sediment motion under unidirectional current, *Sedimentology*, 24, 507–527.
- Nielsen, P. (1986), Suspended sediment concentrations under waves, *Coastal Eng.*, 10, 23–31.
- Nielsen, P. (1992), *Coastal Bottom Boundary Layers and Sediment Transport*, 324 pp., World Sci., River Edge, N. J.
- Rose, C. P., and P. D. Thorne (2001), Measurements of suspended sediment transport parameters in a tidal estuary, *Cont. Shelf Res.*, 21, 1555–1575.
- Sheng, J., and A. E. Hay (1995), Sediment eddy diffusivities in the near-shore zone, from multifrequency acoustic backscatter, *Cont. Shelf Res.*, 15, 129–147.
- Sleath, J. F. A. (1984), *Sea Bed Mechanics*, 355 pp., John Wiley, Hoboken, N. J.
- Smith, J. D. (1977), Modeling of sediment transport on continental shelves, in *The Sea*, vol. 6, edited by E. D. Goldberg et al., pp. 539–577, John Wiley, Hoboken, N. J.

- Thorne, P. D., P. J. Hardcastle, and R. L. Soulsby (1993), Analysis of acoustic measurements of suspended sediments, *J. Geophys. Res.*, *98*, 899–910.
- Van Rijn, L. C. (1984), Suspended transport, part II: Suspended load transport, *J. Hydrol. Eng.*, *110*, 1613–1641.
- Vincent, C. E., and A. Downing (1994), Variability of suspended sand concentrations, transport and eddy diffusivity under non-breaking waves on the shore face, *Cont. Shelf Res.*, *14*, 223–250.
- Vincent, C. E., and P. D. Osborne (1995), Predicting suspended sand concentration profiles on a macro-tidal beach, *Cont. Shelf Res.*, *15*, 1497–1514.
- Webb, M. P., and C. E. Vincent (1999), Comparison of time-averaged acoustic backscatter concentration profile measurements with existing predictive models, *Mar. Geol.*, *162*, 71–90.
- Yalin, M. S. (1963), An expression for bed-load transportation, *J. Hydrol. Div.*, *89*, 221–250.
-
- W. B. Dade, Department of Earth Sciences, Dartmouth College, Fairchild Hall HB 6105, Hanover, NH 03755, USA. (w.brian.dade@dartmouth.edu)
- C. T. Friedrichs, Virginia Institute of Marine Science, College of William and Mary, P. O. Box 1346, Route 1208, Greates Road, Gloucester Point, VA 23062, USA. (cfried@vims.edu)
- G. Lee, Korea Ocean Research and Development Institute, 1270 Sadong, Ansan 425-744, Korea. (glee@kordi.re.kr)
- C. E. Vincent, School of Environmental Sciences, University of East Anglia, Norwich NR4 6TJ, UK. (c.vincent@uea.ac.uk)